Received: 13 January 2021 | Revised: 20 January 2021 | Accepted: 21 January 2021

DOI: 10.1002/hon.2840

WILEY

ORIGINAL RESEARCH ARTICLE

FZD6 triggers Wnt–signalling driven by WNT10B^{IVS1} expression and highlights new targets in T-cell acute lymphoblastic leukemia

Adriana Cassaro[1,2] | Giovanni Grillo[2] | Marco Notaro[3] | Jessica Gliozzo[3] | Ilaria Esposito[1] | Gianluigi Reda[4] | Alessandra Trojani[2] | Giorgio Valentini[3] | Barbara Di Camillo[5] | Roberto Cairoli[2] | Alessandro Beghini[1]

[1]Department of Health Sciences, University of Milan, Milan, Italy

[2]Department of Oncology, Hematology Unit, Niguarda Hospital, Milan, Italy

[3]Department of Computer Science "Giovanni degli Antoni", University of Milan, Milan, Italy

[4]Department of Oncology, Hematology Unit, Ospedale Maggiore Policlinico, Milan, Italy

[5]Information Engineering Department, University of Padova, Padova, Italy

Correspondence
Alessandro Beghini, Department of Health Sciences, University of Milan, Via Di Rudinì 8, Milan 20142, Italy.
Email: alessandro.beghini@unimi.it

Funding information
Fondazione Regionale per la Ricerca Biomedica, Grant/Award Number: FRRB 2015; Novartis Pharma, Grant/Award Number: 2017; LGK974 Drug Supply; Lions Club Milano Host, Grant/Award Number: 2017

Abstract

Wnt/Fzd signaling has been implicated in hematopoietic stem cell maintenance and in acute leukemia establishment. In our previous work, we described a recurrent rearrangement involving the WNT10B locus (WNT10B^{R}), characterized by the expression of WNT10B^{IVS1} transcript variant, in acute myeloid leukemia. To determine the occurrence of WNT10B^{R} in T-cell acute lymphoblastic leukemia (T-ALL), we retrospectively analyzed an Italian cohort of patients (n = 20) and detected a high incidence (13/20) of WNT10B^{IVS1} expression. To address genes involved in WNT10B molecular response, we have designed a Wnt-targeted RNA sequencing panel. Identifying Wnt agonists and antagonists, it results that the expression of *FZD6*, *LRP5*, and *PROM1* genes stands out in WNT10B^{IVS1} positive patients compared to negative ones. Using MOLT4 and MUTZ-2 as leukemic cell models, which are characterized by the expression of WNT10B^{IVS1}, we have observed that WNT10B drives major Wnt activation to the FZD6 receptor complex through receipt of ligand. Additionally, short hairpin RNAs (shRNAs)-mediated gene silencing and small molecule-mediated inhibition of WNTs secretion have been observed to interfere with the WNT10B/FZD6 interaction. We have therefore identified that WNT10B^{IVS1} knockdown, or pharmacological interference by the LGK974 porcupine (PORCN) inhibitor, reduces WNT10B/FZD6 protein complex formation and significantly impairs intracellular effectors and leukemic expansion. These results describe the molecular circuit induced by WNT10B and suggest WNT10B/FZD6 as a new target in the T-ALL treatment strategy.

KEYWORDS
FZD6, LGK974, porcupine inhibitor, T-ALL, Wnt signaling, WNT10B

1 | INTRODUCTION

Acute T-lymphoblastic leukemia (T-ALL) is an uncommon hematological malignancy, arising from the proliferation of immature T-cell precursors or lymphoblasts in bone marrow and other organs occurring to 15% of pediatric and 25% of adult ALL.[1–3]

Normal T lymphocyte development occurs mostly in the thymus and depends on the lifelong seeding of hematopoietic progenitors that originate in the bone marrow.[4,5] Thymocyte differentiation in the thymus is tightly regulated by a number of molecular pathways, one of which increasingly recognized for T cell development, being the Wnt/β-catenin signaling cascade.[6] In the hematopoietic system, a role for Wnt signaling is first demonstrated during T cell development in the thymus where it provides proliferation signals to immature thymocytes.[7] Although the physiologic role of Wnt signaling in post-thymic T cell development remains poorly defined, data indicate that Wnt can regulate the stemness of $CD8^+$ T cells by suppressing their differentiation into Teff cells.[8] In summary, Wnt proteins are secreted glycoproteins that bind to a receptor complex comprising the cysteine-rich domain (CRD) of a seven-transmembrane Frizzled (FZD) receptor family member and a co-receptor of the low-density lipoprotein receptor-related protein LRP-5 or LRP-6.[9,10] In the canonical Wnt pathway, WNT-FZD complex has been reported to emanate an intracellular signaling leading to N-terminally dephospho-β-catenin (active β-catenin, ABC) that results in β-catenin breakdown inhibition and its recruitment to the plasma membrane as an early response to WNT stimulation.[11,12] Subsequently, β-catenin is routed to the nucleus, where it selectively interacts with the factors such as T cell factor (TCF)/lymphoid enhancer factor (LEF) and is then recruited, through enhancers, to chromatin acting as transcriptional co-activators of Wnt-regulated genes.[13] Recent models highlight the complex nature of Wnt-mediated gene regulation underlining that β-catenin is not sufficient for gene target activation (https://web.stanford.edu/group/nusselab/cgi-bin/wnt/target_genes).[14,15] Altered expression levels of Wnt signaling components have been closely related to initiation and progression of acute and chronic leukemia.[16–18] The highest level of active Wnt signaling is detected in the most immature $CD4^-CD8^-$ (double negative, DN) cells by differential expression, which is determined by elevated levels of activating and lower levels of inhibiting factors in the Wnt signaling cascade.[19] WNT ligands may also regulate T-cell mediated immune responses by secreted factors that stimulate bone formation and hemopoietic cells,[20] one of them being WNT10B.[21] In the thymus, loss- and gain-of-function studies have indicated that at least two stages of thymopoiesis require Wnt/β-catenin signaling, specifically WNT5B and WNT10B are expressed at high levels in the single positive (SP) thymic subsets.[19,22] The prevalent influence of secreted Wnt signaling proteins in hematopoiesis[22–24] has renewed efforts to determine the role of Wnt signaling to leukemia establishment. Only recently it has been demonstrated by experimental evidence that oncogenic growth in leukemias of both myeloid and lymphoid lineages is dependent on Wnt signalling.[16,25–28] The role of Wnt-signalling in leukemia stem-cell biology has been emphasized in mouse models of T-ALL.[25,26,29] Activated β-catenin in thymocytes confers genomic instability, thus promoting RAG-dependent T-cell lymphomas.[30] Over 80% of childhood T-ALL patients showed upregulated CTNNB1 (β-catenin) gene, and its suppression by siRNA of the expression led cells to apoptosis in vitro.[16] The clinical outcome remains poor due to frequent relapse and drug resistance,[2,3] and this poor outcome is mainly caused by a subpopulation of chemotherapy-resistant leukemic cells with stem cell-like properties, named 'leukemia initiating cells' (LICs). Expression of $CD34^+/CD4^-$ or $CD34^+/CD7^-$ discriminates subfractions of cells with long-term repopulating ability in childhood T-ALL.[31] More recent evidence to support a causative role for Wnt signaling reported that Wnt-active cells comprise only a small minority, highly enriched for LICs, of the bulk leukemia cell population in the BM of mice with clinically morbid T-ALL disease.[26] Preliminary data in our laboratory have shown that $WNT10B^{IVS1}$ variant, described in AML,[27] is expressed also in T-ALL patients.[32] To further investigate a role for this critical signaling pathway in human T-ALL, we analyzed a multicentric Italian cohort of patients ($n = 20$) diagnosed as T-ALL, with $WNT10B^{IVS1}$ expression being observed in 13 patients. We also confirm the relevance of these findings to human disease by detecting the molecular circuit triggered by WNT10B over-expression using the MOLT-4 and MUTZ2 cell models that express the $WNT10B^{IVS1}$ allele variant. Several pharmacologic compounds have been developed to disrupt Wnt/β-catenin signaling with the endpoint to interfere with the activated canonical Wnt signaling.[33,34] We employ here a selected Porcupine (PORCN) inhibitor, the small molecule LGK974,[34] and TGFβRI inhibitor A83-01 showing to down-regulate FZD6.[35] PORCN is specific to Wnt post-translational acylation, which is required for subsequent WNT ligands secretion.[36] Inhibiting the activity of PORCN leads to suppression of Wnt ligand-driven signaling activity in several models.[37,38] In this report, we examine the expression of the Wnt signaling cascade components mediated by WNT10B and the effects of specific gene silencing by short hairpin RNA (shRNA), as well as the exposure to the potent PORCN inhibitor (LGK974), or the TGFβRI inhibitor (A83-01) on the WNT10B-mediated Wnt signaling activation. These findings could provide a strategy to eliminate the Wnt-active subpopulations within bulk leukemia cells highly enriched for LICs by targeting Wnt-driven molecular targets.

2 | MATERIALS AND METHODS

2.1 | Patients and cell lines

The study included 20 untreated primary T-ALL patients diagnosed between 2004 and 2019 and three healthy donors. All the samples were obtained from the Department of Hematology, Niguarda Ca' Granda Hospital and from Policlinico Hospital of Milan, and they were processed as approved by the Institutional Review Board (N°19-22.06.2018). Each patient and donor gave his/her informed consent in accordance with the Declaration of Helsinki for collection of clinical data, the cryopreservation of bone marrow samples and

the performance of DNA/RNA-analysis for scientific purposes, in accordance with institutional guidelines. Bone marrow samples from each patient were collected and cryopreserved at diagnosis and then centrally analyzed at the Department of Health Sciences - University of Milan, Italy. HeLa (ATCC CCL-2) and MOLT-4 (ATCC CRL-1582) cells were grown in DMEM (Gibco) medium containing Glutamax and RPMI (Gibco), respectively. MUTZ-2 (DSMZ ACC 271) cells were grown in 60% alpha-MEM (Gibco) medium, complemented with 20% fetal bovine serum, 20% conditioned medium from 5637 cell line (DSM ACC 35), 1% penicillin/streptomycin and 50 ng/ml SCF (STEM CELL Technologies). Cell lines were routinely tested to exclude *mycoplasma* contamination.

2.2 | Cell based assays

MOLT-4 cell line was treated with LGK974 and A83-01 inhibitors and recombinant human Wnt-10B. LGK-974 was kindly provided by Novartis (Bâsel, Switzerland), while A83-01 and rhWnt-10B were purchased from Tocris Bioscience and R&D System respectively. Apoptosis was assessed by labeling cells with eBioscience™ Annexin V-FITC Apoptosis Detection Kit (ThermoFisher Scientific) and finally analyzed by flow cytometry on a FACSVerse (BD Biosciences). EdU assays for HeLa cells were performed using Click-It EdU imaging kit C10337 (ThermoFisher Scientific) adding 10 μM EdU 3 h prior fixation. Images were obtained with a ZEISS Upright Axio Imager Z1 motorized Microscope, with EC Plan-Neofluar 10× and 20× objective and AxioCam MRm camera. We used the Axiovision Rel 4.7 software. Cell proliferation was evaluated by flow cytometry analysis after EdU incorporation into DNA using Click-iT™ EdU Alexa Fluor™ 488 Flow Cytometry Assay Kit (ThermoFisher Scientific). Relative cell proliferation was expressed as the percentage of EdU Alexa Fluor™ 488 median fluorescence of treated cells compared to that of cells treated with the specific vehicle. The viability of MOLT-4 and MUTZ-2 cells after concentration- and time-dependent treatments was determined using both manual cell count with 0.4% Trypan Blue (Sigma Aldrich) and the standard MTT [3-(4,5-dimethylthiazol-2-yl)-2,5-diphenyltetrazolium bromide] metabolic activity assay (Sigma Aldrich). The viability was expressed as the percentage of optical density of treated cells compared to optical density of cells treated with the specific vehicle. Each experimental condition was done in hexaplicate and repeated at least twice.

2.3 | Transcriptomic analysis

Total RNA was isolated from HeLa, MOLT-4 and MUTZ-2 cells using Quick-RNA™ MiniPrep Plus kit (Zymo Research), following the manufacturer's instructions. Qualitative analysis of RNA was obtained by Bioanalyzer (Agilent Technologies). 1 μg of total RNA was used to reverse transcribe cDNA using ImProm-II™ Reverse Transcriptase (Promega Corporation) followed by PCR endpoint utilizing Platinum™ Hot Start PCR 1X Master Mix, 20% Platinum™ GC Enhancer (Life Technologies, ThermoFisher Scientific). The amplifications of WNT10B/WNT10B^{IVS1} were performed as follows: 94°C for 3min, 30 cycles at 94° for 30 s, 58°C for 30 s, 72°C for 30 s. Real-time qPCR was carried out using the SYBR Fast qPCR master mix (Roche) in the Light Cycler 480 (Roche) according to the manufacturer's protocols. Primer sequences are indicated in Table S1.

2.4 | Next generation sequencing ampliseq analysis

Next generation sequencing (NGS) for RNA analysis was performed on 5 T-ALL and two healthy donors (HD) samples, using a custom 178 gene Ion Ampliseq panel which was based on Ion Ampliseq RNA Wnt signaling panel (ThermoFischer Scientific) with additional amplicons. The additional genes analyzed were: MARK4(NM_001199867), NDP (NM_000266), PROM1(NM_001145847), MLLT11(NM_006818), WNK2(NM_006648), TBL1XR1(NM_024665), ROCK2(NM_004850), LRRFIP2(NM-001134369), USP34(NM_014709). RNA concentration was assessed on Qubit™ 4 fluorometer in combination with Qubit™ RNA HS Assay Kit (Thermofisher Scientific). Library preparation was performed according to the Ion AmpliSeq™ Kit for Chef DL8 protocol (ThermoFischer Scientific # A29024) for automated preparation of libraries per Ion Chef™ instrument. Enriched samples were sequenced on the Ion S5 System Instrument. Sequencing results were preliminary analyzed using Ion Torrent Suite v 5.12.1. Coverage analysis was performed using plugin AmpliSeqRNA v. 5.12.0.1. We examined the differential expression of a total of five patients affected by T-ALL and split them up into two groups (WNT10B^{IVS1}-positive and WNT10B^{IVS1}-negative). Since we had to perform an analysis with few samples for each condition, we needed to find a robust method in this context. In this regard, EdgeR showed to have good performance with a small sample size.[39,40] In particular, the EdgeR exact test suited better than the generalized linear model (glm).[40] Furthermore, it was also recommended to apply a log2FC threshold of 0.5 or 2 to maximize both the quality and the utility of the data by increasing the sensitivity of the tool.[40] Finally, we considered as significantly differentially expressed (SDE) genes those genes having a *p*-value [adjusted with Benjamini-Hochberg (BH) correction] lower than 0.05 and an absolute log2FC value higher than or equal to 2.

2.5 | Droplet digital PCR™

Droplet digital PCR™ (ddPCR) experiments were performed using primers and probes listed in extended Table S1. The 0.1 mM RNA, extracted using the kit Quick-RNA™ MiniPrep Plus kit (Zymo Research), was denatured at 95°C for 5 min and kept on ice prior to addition to the reaction. We performed the experiment on Bio-Rad's QX100 ddPCR system and the reaction mixtures in a final 20 μl volume consisting of 10 μl of 2× One-Step RT-ddPCR Supermix (Bio-Rad), 1 mM Manganese Acetate solution (Bio-Rad), 0.5 μM of primers WNT10B and WNT10B^{IVS1}, 0.25 μM WNT10B_dd1 and

WNT10B^{IVS1}_dd2 probes (Table S1). The 20 µl ddPCR reaction mixture was then loaded into the Bio-Rad DG8 droplet generator cartridge (Bio-Rad). Each well was then filled with 70 µl of droplet generation oil (Bio-Rad), and the prepared cartridge was then loaded into the QX100 droplet generator (Bio-Rad). The thermal cycling conditions consisted of 30 min reverse transcription at 60°C, 5 min initial denaturation at 95°C, followed by 40 cycles of a two-step thermal profile of 30 s denaturation at 94°C and 60 s annealing-elongation at 60°C and a final 10 min denaturation step at 98°C. Plates were finally transferred into the QX 100 droplet reader (Bio-Rad), and ddPCR data were analyzed with QuantaSoft analysis software (version 1.7.4).

2.6 | mRNA in situ detection

Cells were seeded on Lab-Tek II (Nunc) chamber slides and allowed to attach. Subsequently, they were fixed in 3.7% (*w/v*) paraformaldehyde (Sigma Aldrich) in PBS for 15 min at RT. A 50 µl reaction volume was used for each sample, to make the RNA available for reverse transcription, and 0.1M HCl was applied to the cells for 15 min at 37°C. 1 µM of cDNA primer (LNA primer, Exiqon, Qiagen, see Table S2) was added to the sample with 10 U/µl of M-MULV reverse transcriptase (Thermo Scientific), 500 nM of dNTPS (Thermo Scientific), 0.2 µg/µl BSA of (New England Biolabs, NEB) and 1 U/µl of RiboLock RNase Inhibitor (Thermo Scientific) in the 1× M-MULV reaction buffer. Ligation was carried out using 0.1 µM of Padlock Probes with a mix of 0.5 U/µl Ampligase (Epicentre), 0.4 U/µl RNase H (NEB), 1 U/µl RiboLock RNase Inhibitor (Thermo Scientific), Ampligase buffer, 50 mM KCl and 20% formamide. The rolling circle amplification (RCA) was performed with 1 U/µl DNA polymerase (NEB) in the supplied reaction buffer, 1 U/µl RNase inhibitor (Thermo Scientific), 250 µM dNTPS (Thermo Scientific), 0.2 µg/µl BSA (NEB) and 5% glycerol, and its incubation was carried for 90 min. The rolling circle particles (RCPs) were visualized using 100 nM of detection probes (Table S2) in 2× SSC and 20% formamide at 37°C for 20 min. Slides were then washed twice in DEPC-PBS-T, and nuclei were counterstained with 100 ng/ml DAPI (Sigma, D9542). Immunofluorescence images were acquired with a ZEISS LSM510 or ZEISS LSM880 confocal microscope with 20× or 40× oil immersion objectives. We used NIS Elements software for the acquisition and processing of the images.

2.7 | In situ proximity ligation assay

In situ and flow cytometry proximity ligation assay experiments were carried out using Duolink Kits (Sigma Aldrich, # DUO92101 and # DUO94004, respectively). HeLa cells were seeded at a concentration of 1×10^3 cells/well on Lab-Tek II (Nunc) chamber slides. MOLT-4 cells were prepared using cytospin. The cells were fixed with cold 3.7% (*w/v*) paraformaldehyde (PFA, Sigma Aldrich) for 15 min at room temperature (RT) and subsequently permeabilized with 0.1 % Triton X-100. MUTZ-2 cells were fixated with 1% paraformaldehyde and subsequently permeabilized with 0.5% Triton X-100 in PBS+ 1% BSA for 20 min at 4°C. Afterwards the samples were incubated with primary antibodies (mouse WNT10B, ThermoFischer Scientific, 1:100; rabbit FZD4, Abcam, 1:100; rabbit FZD5, Abcam 1:100; rabbit FZD 6, ThermoFischier Scientific, 1:100; Table S3). The subsequent steps of the proximity ligation assay (PLA) (both in situ and flow) followed the manufacturer's instructions. Images were acquired with a ZEISS Upright Axio Imager Z1 motorized Microscope, with EC Plan-Neofluar 20× and 40× oil objectives and AxioCam MRm camera using Axiovision Rel 4.7 software. For quantification, the numbers of RCPs and cell nuclei were counted using CellProfiler (www.cellprofiler.org) on three images. Data analysis of flow-cytometry PLA was performed using FACsVerse, flow cytometry (BD Biosciences).

2.8 | Western blotting

Cells were lysed with an appropriate amount of Nonidet-P40 Cell Lysis Buffer (20 mM Tris HCl, 137 mM NaCl, 10% glycerol, 1% nonidet-P40, 2 mM EDTA) supplemented with complete protease inhibitor and 1 mM PMSF (Cell Signaling Technology) with 1× Phosphatase Inhibitor Cocktail (Cell Signaling Technology). Proteins separated by 10% and 12% SDS gel-electrophoreses were transferred to a polyvinylidene difluoride (PVDF) membrane by semi-dry blotting. The membrane was incubated with primary antibodies against WNT10B (ThermoFisher), β-catenin (BD Transduction Laboratories), ABC-Active β-catenin (Merk Millipore), FZD4 (Abcam), FZD5 (Abcam), FZD6 (ThermoFisher Scientific), GAPDH (Abcam) at 4°C for 2 h (Table S3).

2.9 | Co-immunoprecipitation experiments

Co-IP was done using magnetic protein A beads (Dynabeads™ Protein A, Invitrogen) following the manufacturer's instructions. For 500 µg of total protein extracted, 50 µl of magnetic protein A beads were used, and antibodies, diluted 1:100 in PBS/Tween20 0.02%, were added to the beads. The samples were incubated 20 min at room temperature while rotating and being washed three times with PBS. Proteins were eluted off the beads by adding 30 µl of 3× SDS sample buffer (added with 1/10 dithiothretol), heated 5 min at 95°C and finally analyzed by immunoblotting.

2.10 | Cell manipulations and treatments

RNAi experiments were carried out by using shRNA targeting vectors from Sigma Aldrich. The details of the nucleotide sequences used for RNA-interference are given in Table S4. The recombinant lentivirus was produced by the insertion of shRNA of WNT10B into pLKO-puro vector, and the ligation reactions were transformed into Stbl3 (Life Technologies) chemically competent. E. coli pLKO constructs were

used to make lentivirus in HEK293T cells with a polyethylenimine (PEI) transfection protocol. At 24h post-transfection, media was changed to the target cell media (without antibiotics). HEK293T cells were returned to 37°C for 48 h to produce viral particles. Viral media was then collected and filtered to infect HeLa and MOLT-4 cells. Infected cells were incubated for 48–72 h and then given fresh growth media for 24–48 h before beginning the selection by puromycin.

2.11 | Statistical analysis

Data are presented as mean ± SEM or ratios among treated and controls, in independent experiments as indicated in the Figure legends. Statistical significance of differences between experimental groups and controls was assessed by two-tailed unpaired *t*-test. *p* values < 0.05 were considered as statistically significant.

3 | RESULTS

3.1 | WNT10B^{R} rearrangement associates with T-ALL patients

In our previously reported study, we identified a recurrent rearrangement of WNT10B (WNT10B^{R}) leading to expression of the transcript variant WNT10B^{IVS1} in a cohort of AML patients with intermediate/unfavorable risk.[16] In a preliminary analysis including a small subset of T-ALL patients, we reported that WNT10B^{R} was significantly overexpressed.[32] Taking into consideration these previous results, in this report, we evaluated the presence of WNT10B/WNT10B^{IVS1} expression in bone marrow mononuclear cells (BMNCs) derived from a cohort of newly diagnosed T-ALL patients ($n = 20$) and healthy donors ($n = 3$). Consistent with previously published data, WNT10B is expressed at low level in normal BM[16,24–27], and WNT10B^{IVS1} results undetectable, conversely WNT10B^{IVS1} transcript was detected in 13 out of 20 T-ALL patients (Figure 1A; Table 1). To address relevant expression pattern in Wnt pathway transcriptome, we performed AmpliSeq transcript analyses (GSE159797) of BMNCs from T-ALL patients ($n = 5$) and healthy donors ($n = 2$). AmpliSeq transcriptome reproducibility enables a highly accurate detection for differential gene expression analysis in a relatively small sample set, in particular for highly expressed genes, without the need for data normalization algorithms. The overall number of detectable RNAs does not significantly differ between WNT10B^{IVS1}-positive and WNT10B^{IVS1}-negative patients, but individual genes differ in expression level between the two groups of patients (Figure 1B). Genes ($n = 23$) with prominent expression differences are listed in Figure 1C. Genes higher expressed in WNT10B^{IVS1}-positive than in WNT10B^{IVS1}-negative include PLCB4, PROM1, FZD6, LRP5, PLAU and MLLT11 (Figure 1D). Additional genes more robustly expressed in WNT10B^{IVS1}-positive include TBL1XR1, CTNND1, and VANGL1. Conversely, a number of genes showed a lower expression level in WNT10B^{IVS1}-positive patients including PPP2R2B, WNT7A, CAMK2D, PRKCA, FZD3 and WNT11 (Figure 1D). Although the number of patients analysed is limited, the results suggest a context of significant Wnt signaling activation in WNT10B^{IVS1}-positive patients.

3.2 | Expression and proximity ligation analyses reveal a WNT10B-FZD6 circuit in MOLT-4 cell line

To assess the role of WNT10B^{IVS1} in the WNT signaling activation, we have recently investigated the WNT10B ligand expression among several cell lines (Figure 2A), revealing the expression of WNT10B^{IVS1} in MOLT-4 T-ALL cell line and MUTZ-2 AML cell line versus HeLa cells, a cell line used as technical control, and characterized by the unique over-expression of WNT10B (Figure 2A). Consistent with RT-PCR analysis, one-step Droplet Digital PCR (Figure 2B upper panel) and mRNA in situ detection (Figure 2B lower panel), using WNT10B/WNT10B^{IVS1} probes, have shown the exclusive expression of WNT10B^{IVS1} in MOLT-4 cell model.

A relevant question is which FZD receptor/s binds WNT10B ligand in the MOLT-4 cell model, pointing to an impact on functional significance. This question has been addressed employing co-immunoprecipitation assay by using antibodies against FZD4/5/6 receptors, previously evaluated by gene expression analysis (Figure 2C), and followed by immunoblotting with antibody against WNT10B (Figure 2D). We have thus revealed a high signal for WNT10B/FZD6 interaction, a weak signal for WNT10B/FZD4 and WNT10B/FZD5 interactions (Figure 2D), as expected following expression analyses (Figure 2C). These results are confirmed using Proximity Ligation Assay (PLA) for FZD 4/5/6 and WNT10B molecule. We detected rolling cycle amplification products (RCPs) by PLA only for WNT10B/FZD6 ligand/receptor interaction (Figure 2E,F), suggesting that FZD6 acts as a master receptor for WNT10B ligand in MOLT-4 cell model.

3.3 | WNT10B^{IVS1} gene silencing impairs WNT10B/FZD6 interaction in MOLT-4 cells

To assess the mechanistic insights of the WNT10B autocrine signaling, we pointed out the consequence of WNT10B/WNT10B^{IVS1} knockdown. Silencing of the WNT10B gene in MOLT-4 cell line, by shWNT10B^{IVS1}1 and shWNT10B^{IVS1}2 molecules, results in a specific decreased expression of WNT10B^{IVS1} transcript and, as we highlighted, with higher silencing efficiency by shWNT10B^{IVS1}2, using the mRNA in situ detection approach (Figure 3A,B). Paralleling the above findings, WNT10B^{IVS1} knockdown generates an expression down-modulation of Wnt signaling effector genes (i.e. CTNNB1, AXIN2, PYGO2, GSK3β) (Figure 3C), suggesting a functional role that needs further investigation. Consistent with the transcriptome results, after due to WNT10B^{IVS1} knockdown, even the WNT10B-FZD6 ligand–receptor interaction resulted in a statistically significant down modulation ($p < 0.0001$) visualized as RCPs decrease (Figure 3D,E).

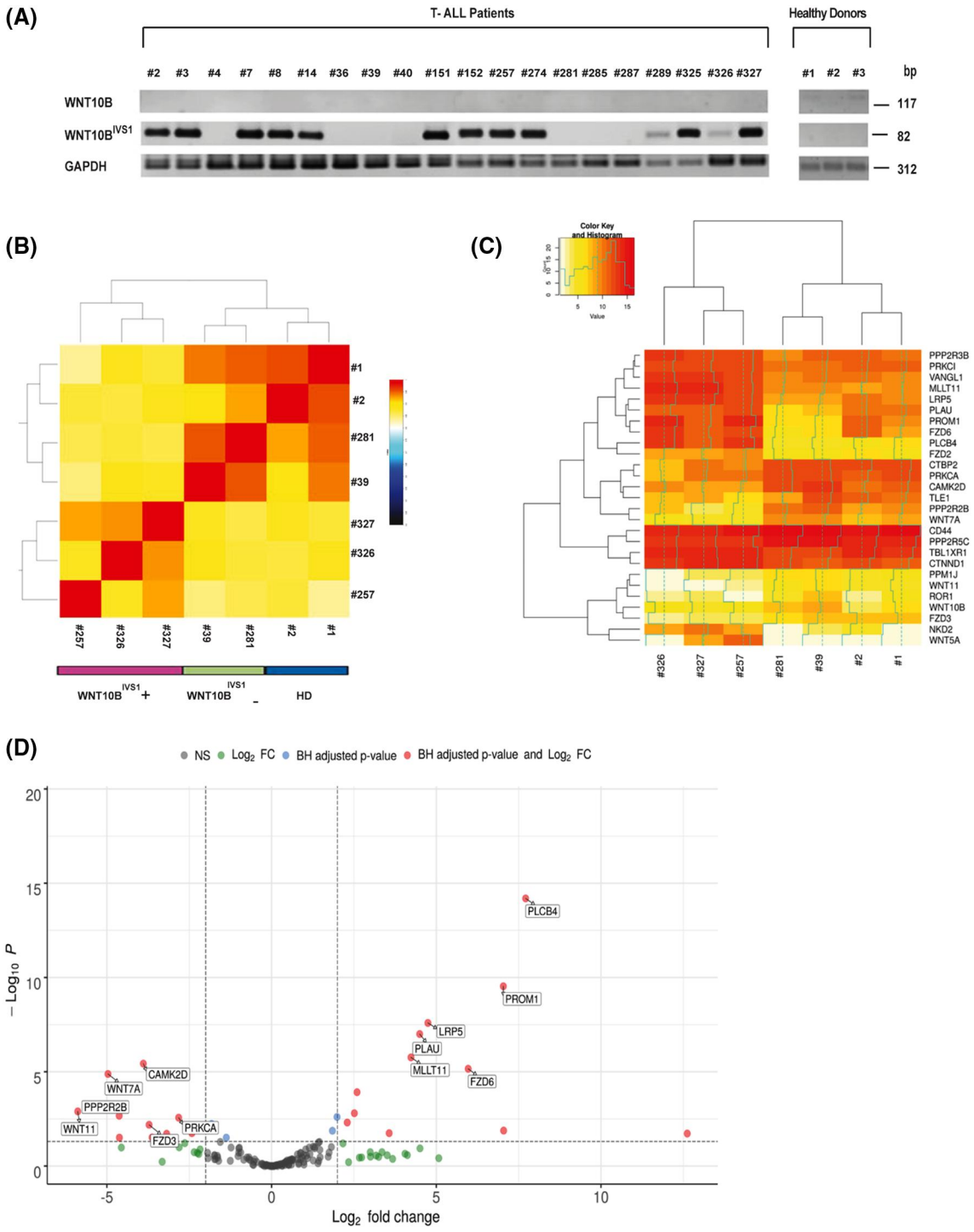

FIGURE 1 WNT-targeted gene expression analysis in T-ALL between WNT10B^{IVS1}-positive and WNT10B^{IVS1}-negative subjects. (A) RT-PCR analysis of WNT10B, WNT10B^{IVS1} and GAPDH transcripts, respectively, in T-ALL samples (n = 20) and lymphocytes from aged-matched healthy donors (n = 3). (B) Correlation heatmap between samples from T-ALL WNT10B^{IVS1}-positive patients (n = 3), T-ALL WNT10B^{IVS1}-negative patients (n = 2) and healthy donors (n = 2). (C) The heatmap shows the differentially expressed genes in the two groups considering only those with an adjusted p-value <0.05 and a |log2FC| ≥2. Samples (columns) and genes (rows) are clustered using hierarchical clustering. The heatmap depicted shows the 23 significantly differentially expressed genes (SDE) for each considered sample, and intensity indicates the ratio of mRNA expression. PLCB4, FZD6, PROM1, PLAU and LRP5 expression stand out in WNT10B^{IVS1}-positive samples whereas PPP2R2B, WNT11, WNT7A, PRKCA, and CAMK2D are highly down-regulated in the same group. (D) Volcano plot for the pair WNT10B^{IVS1}+ versus WNT10B^{IVS1}- (p value vs. fold change ratio) shows the SDE genes highlighted in red dots (genes with BH adjusted p-value ≤0.05 and a log2FC ≥ 2). The top six up- and down-regulated genes are identified as shown according to the false discovery rate (FDR). The horizontal dotted line corresponds to p-value = 0.05 and the two vertical dotted lines to log2FC = ±2

TABLE 1 Patient and disease characteristics

	All (n = 20)	WNT10B^{IVS1} positive (n = 13)	WNT10B^{IVS1} negative (n = 7)
Age at diagnosis			
Median (range), years	32 (19–59)	33 (21–59)	28 (19–59)
≥40 years, n (%)	6 (30)	4 (29)	2 (33)
Male, n (%)	12 (60)	7 (50)	5 (83)
Hyperleukocytosis at diagnosis (WBC >100 × 10^9/L), n (%)	6/18 (33)	4/12 (33)	2/6 (33)
Immunophenotypic subtypes, n (%)			
Pro-T-ALL	2/18 (11)	2/13 (15)	0/5 (0)
Pre-T-ALL	12/18 (67)	7/13 (54)	5/5 (100)
Cortical T-ALL	4/18 (22)	4/13 (31)	0/5 (0)
Medullary T-ALL	0/18 (0)	0/13 (0)	0/5 (0)
Cytogenetic subgroups, n (%)			
Normal karyotype	6/18 (33)	5/12 (42)	1/6 (17)
MLL aberrations	2/18 (11)	1/12 (8)	1/6 (17)
Complex karyotype	1/18 (5)	1/12 (8)	0/6 (0)
Other abnormalities	9/18 (50)	5/12 (42)	4/6 (67)
Response after first line therapy (complete remission), n (%)	17/19 (89)	11/13 (85)	6/6 (100)
Relapse/progression after first line therapy, n (%)	6/19 (32)	4/13 (31)	2/6 (33)
Allogeneic HSCT, n (%)	12/19 (63)	7/13 (54)	5/6 (83)
Relapse/progression after allogeneic HSCT, n (%)	3/12 (25)	2/7 (28)	1/5 (20)

Abbreviations: HSCT, hematopoietic stem cell transplantation; WBC, white blood cell.

To determine the specificity of our silencing assay, WNT10B knockdown has been performed on HeLa cell line by using the shWNT10B molecule. In this case, we observed a decrease of WNT10B transcript in situ (Figure S1A,B) and a down modulation of the WNT effector genes (Figure S1C). Silencing of WNT10B transcript in HeLa cells also produces a significant decrease ($p < 0.0001$) of WNT10B-FZD6 RCPs (Figure 1D,E) as well as in MOLT-4 cell line. In parallel with the above results, WNT10B^{IVS1} knockdown in MOLT-4 cells ensues a strong decrease of cell proliferation potential (Figure 3F–H), as well as WNT10B knockdown in HeLa cells (Figure S1F–H).

3.4 | Porcupine inhibitor LGK974 decreases WNT10B-mediated autocrine Wnt signaling activation and affects transcript stability

Parallel down-modulation of WNT10B^{IVS1} and WNT10B transcripts in MOLT-4 and HeLa cell lines, respectively, raised translational implications of the porcupine inhibitor treatment to interfere with the autocrine WNT10B overexpression. The consequence of the treatment with porcupine inhibitor is defined by the inhibition of Wnt acyl-transferase activity. It was demonstrated that the IC_{50} of LGK974 inhibitor is 0.3 nM in HN30 cell line; nevertheless, in several cell types, inhibition of Wnt signaling requires concentrations up to 5 μM.[34] We evaluated the effects of increasing concentration of LGK974 inhibitor (0.1, 0.5, 1.0, 1.5, 2.0 and 5.0 μM) on Wnt signaling activation in MOLT-4 cell model. LGK-974 treatment, at different concentrations for 24 and 48 h on MOLT-4 cell line, resulted in a dose-dependent decrease of WNT10B-FZD6 ligand–receptor interactions (Figure 4A–C). We herewith observe that LGK974 decreases total and active-β-catenin level dose-dependently (Figure 4D), as well as expression of other Wnt effectors (Figure 4E). Importantly, in parallel with these results, we find that LGK-974 treatment strongly down-modulate the WNT10B^{IVS1} expression, pointing out the ability of this porcupine inhibitor to interfere with WNT10B ligand and transcript stability (Figure 4C,E). Notably, we have obtained almost the same WNT10B^{IVS1} knock-down expression already at the lowest LGK-974 concentration, such as previously obtained by WNT10B^{IVS1} silencing, thus supporting the hypothesis of a negative post-transcriptional feedback circuitry. In parallel with the above results, LGK-974 inhibitor treatment reduced the MOLT-4 cell viability in a dose- and time-dependent manner, as we assessed by manual cell count with Trypan blue and MTT assay (Figure 4F,G). Furthermore, LGK-974 treatment produces a reduction of cell proliferation potential of MOLT-4 cell line as measured by EdU cell proliferation assay (Figure S2A). This is accompanied by a slight increase in apoptosis rate at 96 h, as shown in Figure 4H. In order to confirm that the observed effects were not merely specific for MOLT-4 cells lines, but undoubtedly ascribed to the suppressive

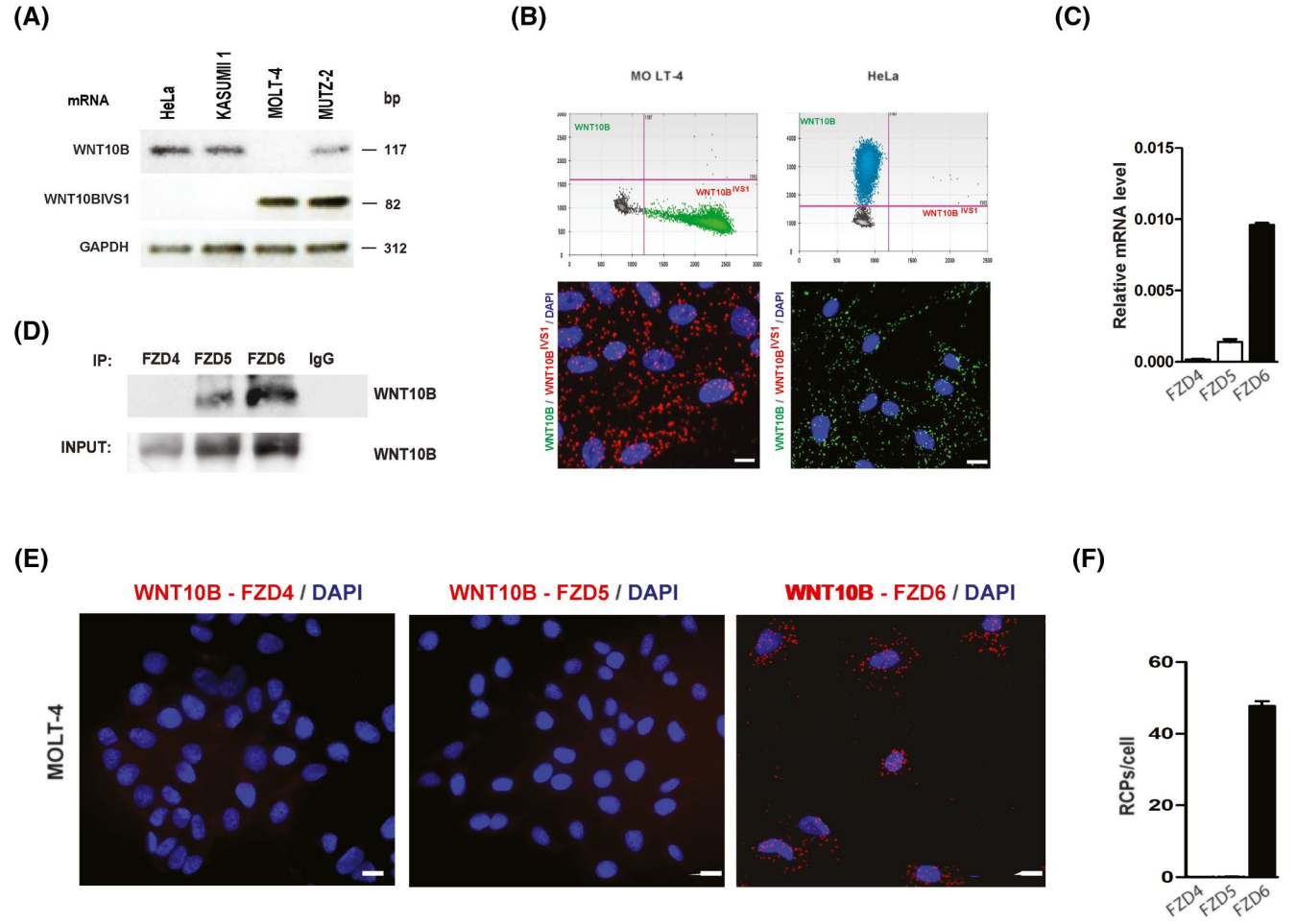

FIGURE 2 WNT10B expression and receptor interactions in different leukemia cell lines. (A) RT-PCR analysis of WNT10B and WNT10B^{IVS1} in the indicated cell lines. (B) qPCR analysis of FZD4, FZD5, and FZD6 expression in MOLT-4 cell line. (C) Upper panel: detection of WNT10B-WNT10B^{IVS1} expression by droplet digital PCR (ddPCR) assay, using two different fluorophores in Taqman™ assays (FAM and VIC). The FAM and VIC fluorescence for each droplet is plotted as a data point on each graph. The droplet threshold for each fluorophore used is indicated by the magenta lines, determining whether a droplet is considered positive or negative for either FAM or VIC fluorescence. In the lower panel representative images and quantification of WNT10B-WNT10B^{IVS1} (green and red dots) mRNA in situ detection in human cultured HeLa and MOLT-4 cells. Scale bar, 10 μm. Cell nuclei are shown in blue. (D) WNT10B-FZD4, WNT10B-FZD5 and WNT10B-FZD6 protein complexes detection by co-immunoprecipitation assay (Co-IP). (E) Proximity ligation assays (PLA) with antibodies against WNT10B and FZD4, FZD5 and FZD6 of MOLT-4 cell line. Red fluorescence dots resulting from the juxtaposition of anti-WNT10B and anti-FZDs antibodies were visualized by fluorescence microscopy with concomitant DAPI nuclear staining. Scale bar, 10 μm. (F) Representative quantification of the number of dots per cell

effect of LGK-974 on WNT10B-mediated Wnt signaling activation, additional experiments were conducted using the MUTZ-2 leukemic cell line, characterized by the expression of WNT10B^{IVS1}, with an increasing concentration of LGK974 (Figure S3). We therefore show that FZD6 is the most expressed receptor in MUTZ-2 cell line, among the FZD receptors analysed (Figure S3A), acting as a major specific receptor for WNT10B ligand interaction (Figure S3B,C). LGK974 treatment induces a dose-dependent reduction both of WNT10B-FZDs interaction measured by PLA flow cytometry (Figure S3D), and of total and active-β-catenin levels (Figure S3E). Moreover, we assess that the treatment with LGK974 for 72 h generates a reduction of cell viability (Figure S3F) and an increase of apoptosis in MUTZ-2 cell line (Figure S3G). Furthermore, we examined whether the addition of WNT10B agonist was able to restore the inhibition of Wnt signaling induced by LGK974 treatment in MOLT-4 cell line. When human recombinant WNT10B ligand is added to LGK974-treated MOLT-4 cells, the suppressive effects of LGK974 on cell viability are partially rescued (Figure 5A,B).

3.5 | The TGF-β-inhibitor A83-01 impairs WNT10B-FZD6 interaction by FZD6 down modulation

A previous study showed that TGF-β stimulation increased production of the WNT10B, due to a potential cooperative function for small mother against decapentaplegic (SMAD) and Nuclear

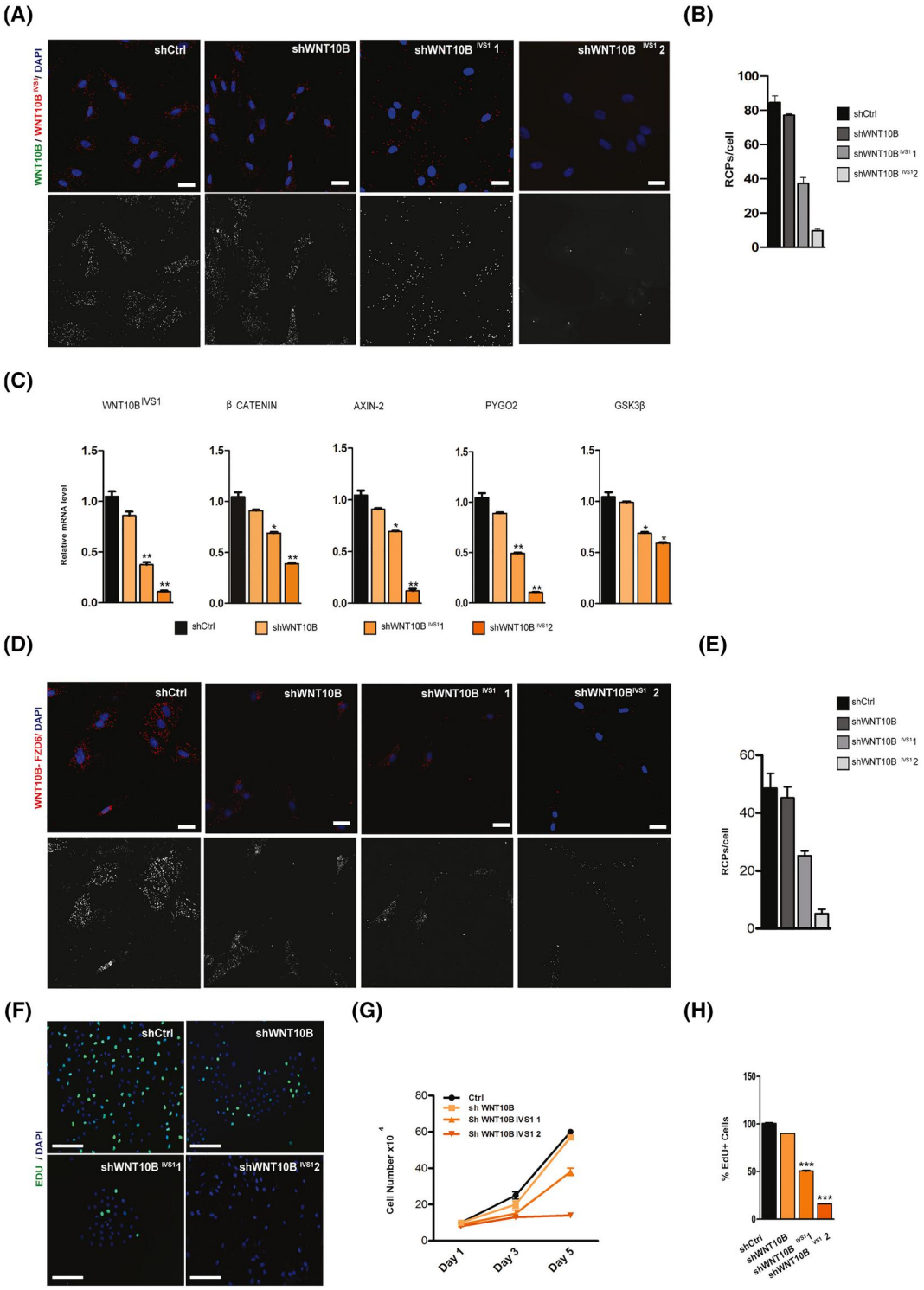

FIGURE 3 WNT signaling is down-modulated by WNT10B^{IVS1} silencing. (A) Upper panel: WNT10B-WNT10B^{IVS1} mRNA in situ detection in human cultured MOLT-4 cells 72 h after infection with WNT10B-WNT10B^{IVS1} silencing lentiviruses (shWNT10B, shWNT10B^{IVS1}1, shWNT10B^{IVS1}2) versus empty vector control (shCtrl). Scale bar, 10 μm. Cell nuclei are shown in blue. Grey scale for dots quantification is represented in the lower panel. Quantification of number of dots per cell is represented in the panel (B). (C) RT-qPCR analysis of the indicated WNT signaling effector genes in MOLT-4 cell line infected with three different WNT10B silencing lentiviruses versus empty vector control (Ctrl). Two-tailed unpaired *t*-test was used for statistical analysis: $^{*}p < 0.05$, $^{**}p < 0.01$, $^{***}p < 0.001$. (D) and (E) WNT10B-FZD6 PLA in human cultured MOLT-4 cells 72 h after infection with WNT10B-WNT10B^{IVS1} silencing lentiviruses [shWNT10B, shWNT10B^{IVS1}1, shWNT10B^{IVS1}2 vs. empty vector control (shCtrl)]. Scale bar, 10 μm. Cell nuclei are shown in blue. Grey scale for dots quantification is represented in the lower panel. In the panel (E) is represented the quantification of number of dots per cell. (F–H) EdU labeling assays of MOLT-4 cell line 72 h after infection with WNT10B-WNT10B^{IVS1} silencing lentiviruses versus empty vector control (shCtrl). Representative images with corresponding quantifications are shown (G) and (H). Scale bar 10 μm

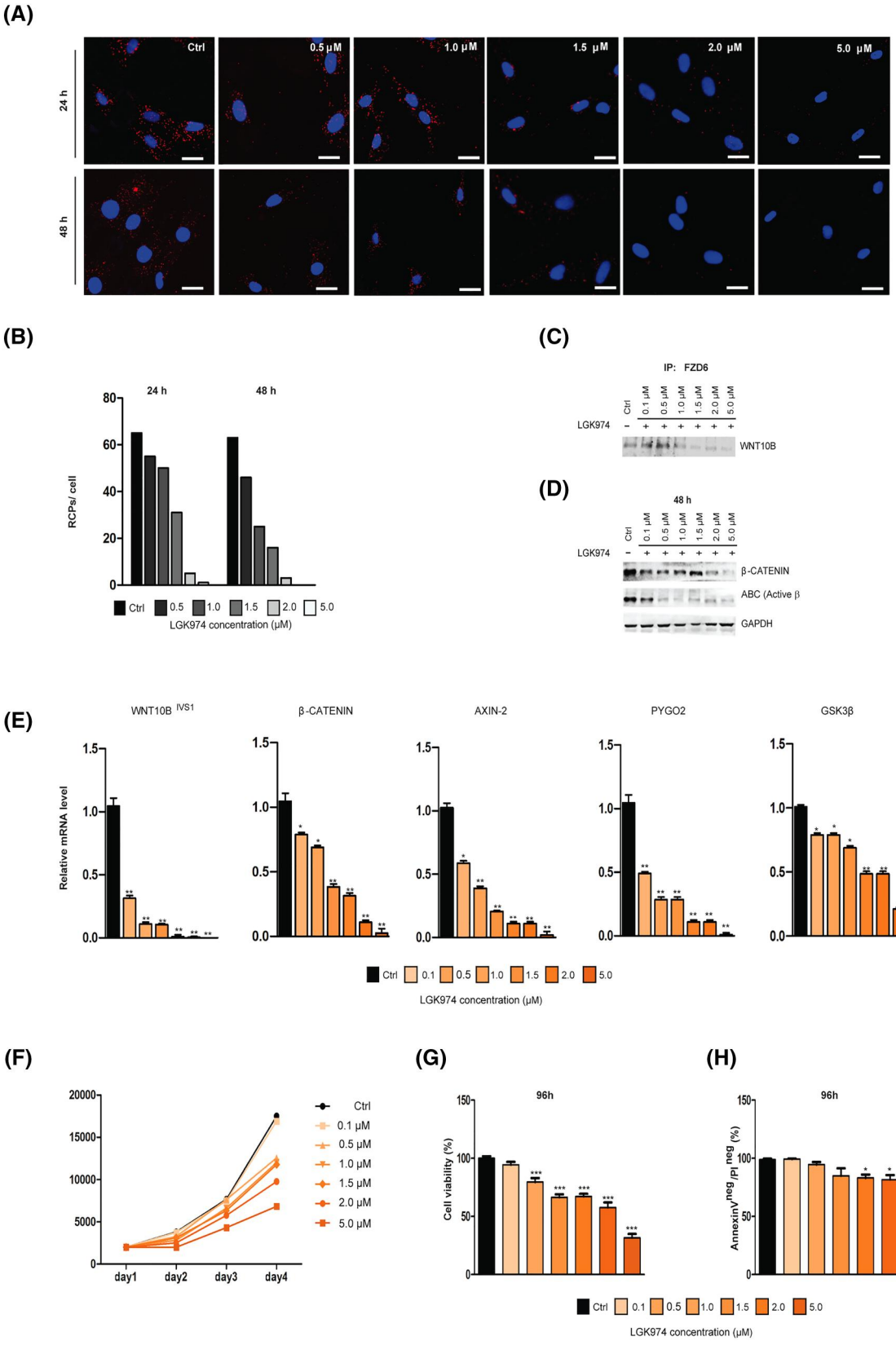

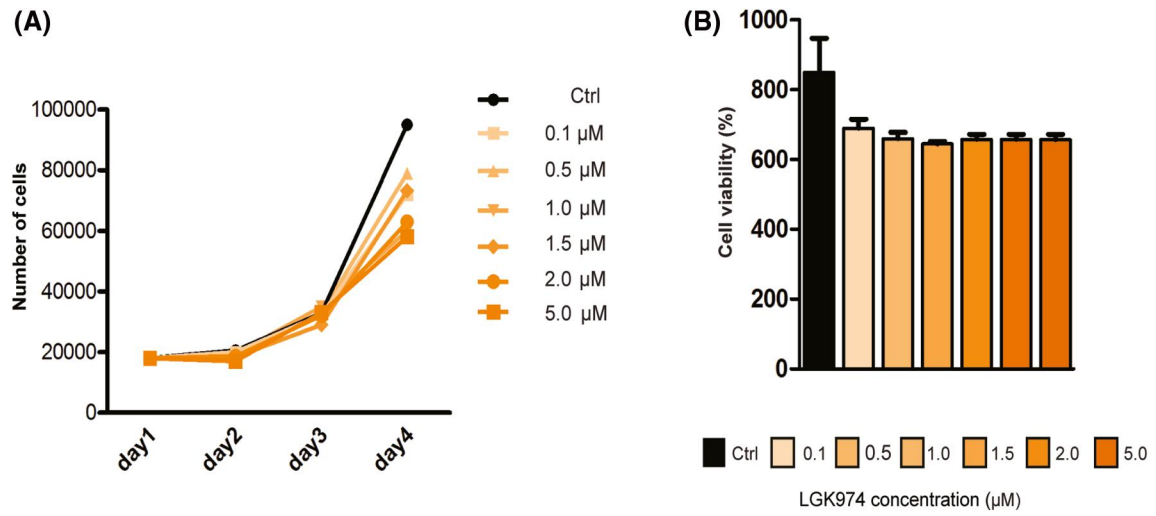

FIGURE 5 Recombinant WNT10B reverse LGK974-mediated effects on MOLT-4 cell line. (A) and (B) MOLT-4 cell line were treated for different endpoints with 100 ng/mL recombinant WNT10B protein and with the increasing concentration of porcupine inhibitor LGK974, and then, cell viability was analysed through Trypan blue cell count (left panel) and MTT assay after 96h of treatment (right panel)

factor of activated T-cells (NFAT) in the induction of WNT10B gene expression.[41] Therefore, taking into consideration this data, we used the small molecule A83-01, a TGF-βRI inhibitor able to down-regulate the FZD6 expression,[35] to modulate the WNT10B-FZD6 interplay via TGF-β signaling pathway. To assess whether the specific FZD6 receptor down-regulation confirms the WNT10B-FZD6 interplay, we perform the PLA experiments after A83-01 exposure at 24 and 48 h, showing a dose-dependent down-modulation of the interaction events visualized as decreasing RCPs (Figure 6A,B). Analysis of the gene and protein expression profiles pointed out the expected down-modulation of FZD6 expression as a consequence of TGF-βRI inhibition after treatment with A83-01 (Figure 6C,D). Conversely, a weak down-modulation of $WNT10B^{IVS1}$ expression or the downstream Wnt effector genes such as *CTNNB1*, *AXIN2*, *PYGO2*, *GSK3*-β (Figure 6D) has been obtained. These data suggest that $WNT10B^{IVS1}$ expression in MOLT-4 cell line is driven by the genomic rearrangement, whereas this is not a consequence of TGF-βRI-mediated induction. Moreover, we notice that MOLT-4 cell viability (Figure 6E,F) and cell proliferation (Figure S2B) are slightly affected by the treatment with A83-01 inhibitor. This is accompanied by an increase in apoptosis rate measured at 96 h (Figure 6G). In parallel with the above results, we demonstrate a significant dose-dependent down-modulation of WNT10B-FZD6 interactions on HeLa cell line over-expressing the WNT10B molecule (Figure S4A,B) as a consequence of FZD6 and WNT10B down-modulation (Figure S4C,D). Furthermore, we showed a consequent reduction of Wnt effector genes, with the exception of GSK-3β, after treatment with A83-01 inhibitor (Figure S4D). It is interesting to note that MOLT-4 cell line showed a better response to treatment with A83-01 inhibitor at lower concentration than in HeLa cells. These results obtained on HeLa cells suggest that without the presence of rearrangement, WNT10B expression would be TGF-βRI-dependent as previously reported.[41]

4 | DISCUSSION

Previous studies have explored the multiple ways abnormal Wnt signaling contributes to the pathogenesis of human leukemia.[16,17,26,27,42–45] Our recent findings also highlight the high prevalence of a *WNT10B* rearrangement (*WNT10B*^{R}), involving intron 1 proximal to the exon 2, and expressing the $WNT10B^{IVS1}$ transcript in acute myeloid leukemia with normal karyotype.[27]

FIGURE 4 WNT10B-FZD6 interaction is down-modulated by treatment with porcupine inhibitor LGK974 in MOLT-4 cell line. (A) PLA in human cultured MOLT-4 cells 24 and 48h after treatment with porcupine inhibitor in a dose-dependent manner. Scale bar, 10 μm. Cell nuclei are shown in blue. In panel (B), the quantification of the number of dots per cell is represented. (C and D) MOLT-4 cells were treated with increasing concentrations of LGK974 inhibitor for 48 h, then was evaluated WNT10B-FZD6 protein complexes detection by co-immunoprecipitation assay (C), and immunoblot analysis for β-catenin and active β-catenin (D) of the same treated cells. (E), RT-qPCR analysis of the indicated WNT signalling effector genes in MOLT-4 cell line after 24h of porcupine inhibitor treatment. Two-tailed unpaired *t*-test was used for statistical analysis: $^{*}p < 0.05$, $^{**}p < 0.01$, $^{***}p < 0.001$. F–G, MOLT-4 cells were cultured with increasing concentrations of LGK974 for different time points; then, cell viability was analyzed through Trypan blue cell count (F) and MTT assay (G). Data are normalized by comparing each condition with DMSO-treated cells. (H) MOLT-4 cell line was treated with LGK974 and then stained with AnnexinV/PI and analyzed through flow cytometry. Data are expressed as the mean ± SEM of three independent experiments. Two-tailed unpaired *t*-test was used for statistical analysis: $^{*}p < 0.05$, $^{**}p < 0.01$, and $^{***}p < 0.001$

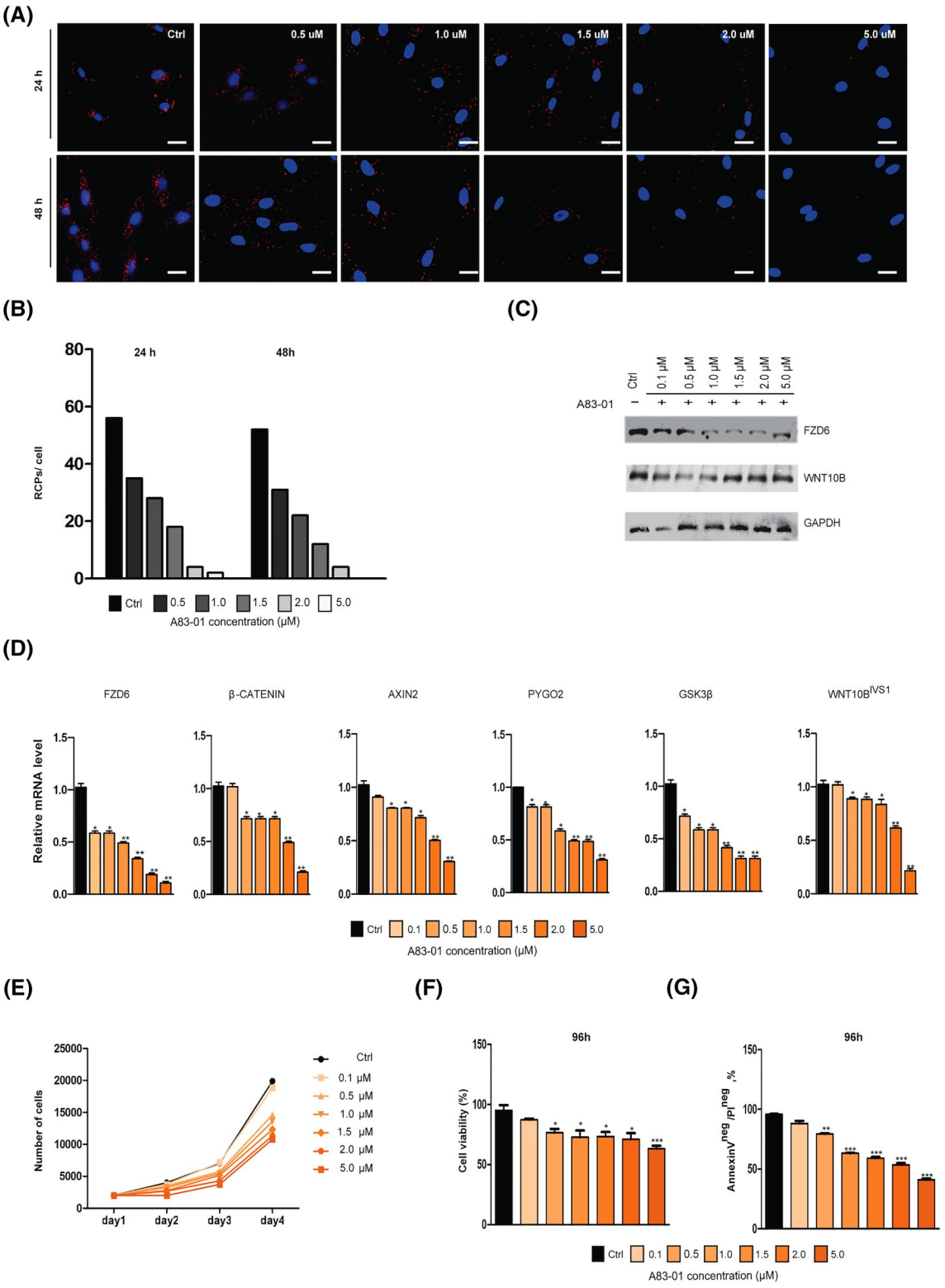

FIGURE 6 TGF-βRI inhibition down-modulates FZD6 expression inhibiting WNT10B-FZD6 interaction. (A) WNT10B-FZD6 PLA in cultured MOLT-4 cells 24 and 48 h after treatment with TGF-βRI inhibitor in a dose-dependent manner. Scale bar 10 μm. Cell nuclei are shown in blue. (B) Quantification of the number of dots per cell. (C) Immunoblot analysis of the same treated cells with antibodies against WNT10B and FZD6 genes and using GAPDH as equal loading control. (D) qPCR analysis of the indicated WNT signaling effector genes in MOLT-4 cell line after 24 h of TGF-βRI inhibitor treatment. Two-tailed unpaired *t*-test was used for statistical analysis. (E and F) Cell viability of MOLT-4 after TGF-βRI inhibitor treatment was analyzed by Trypan blue cell count (left panel) and MTT assay (right panel). Data are represented as mean ± SEM of three independent experiments. Two-tailed unpaired *t*-test was used for statistical analysis: $^{*}p < 0.05$, $^{**}p < 0.01$, $^{***}p < 0.001$. (G) MOLT-4 cells were treated with increasing concentrations of A83-01 inhibitor and then were harvested and stained with Annexin V/PI to analyze cell viability. Data are represented as mean ± SEM of three independent experiments

Based on prior results, it has been suggested the importance of abnormal Wnt activation in T-ALL patients, supported by patients being characterized by a minor subpopulation of Wnt-active cells highly enriched for leukemia-initiating cells (LICs) with both T- and myeloid cell potential.[16,26,31,46] The role played by the Wnt signaling in T-ALL pathogenesis is overly complex and the precise mechanisms underlying leukemia development remain to be elucidated. Paralleling our own observations in an Italian multicentric cohort of newly diagnosed T-ALL patients, we detected a high frequency of WNT10B^{IVS1} expression in bone marrow samples at diagnosis. Analysis of the expression of components and downstream targets of Wnt signaling in a subset of our patient cohort by targeted RNA sequencing technology enables a sensitive detection of significantly differentially expressed (SDE) genes. The data set analysis suggests that the WNT10B^{IVS1}-positive patients shared an active Wnt signaling transcriptional profile delineated by *FZD6*, *PLCB4*, *PROM1*, *LRP5*, *MLLT11* and *PLAU* overexpression, and *WNT7A*, *WNT11*, *PPP2R2B*, *FZD3*, *CAMK2D* and *PRKCA* down-regulation compared to WNT10B^{IVS1} negative patients. Remarkably, these findings support a functional role for *FZD6* in WNT10B^{IVS1} positive patients. *FZD6* was shown drastically increased in B-cell leukemogenesis 47 and in a subset of childhood T-ALL.[16] Furthermore, *PLCB4* overexpression has recently been associated with poor clinical outcome in acute myeloid leukemia,[48] and is linked to T-ALL biology,[49] and *WNT7A* is down-regulated in T-ALL derived cells due to long-term DNA methylation and associated with the WNT canonical pathway upregulation.[50] Of interest is the evidence that lower level of *PRKCA* defines a subgroup of pediatric T-ALL with a very poor outcome.[51] Although the small number of subjects precludes full description of the range of inter-individual divergence in Wnt-genes expression, the use of a highly reproducible RNA assay (AmpliSeq) enables differentially expressed gene discovery from small sample numbers mitigating this limitation to some extent. Further interpretation of our results will require Wnt expression analyses in a larger sample set. This study explores the *WNT10B*^{R}-harboring MOLT-4 T-ALL cell line to examine the molecular cascade induced by WNT10B^{IVS1} overexpression. Although the precise functional role of FZD6 signaling remains unexplored, results in leukemic B cells suggest that up-regulated FZD6 protein is providing canonical pathway signals.[47] The requirement for Wnt ligands in leukemia proliferation suggests the use of specific inhibitors for targeting Wnt secretion.[33,34,38] Wnt ligands require palmitoylation by Porcupine (PORCN) for their secretion and interaction with FZD receptors.[38,52,53] PORCN inhibitors demonstrated a potent and selective interference activity of the Wnt signaling in vivo and in vitro.[33,34] The PORCN inhibitor LGK974 significantly abrogates autocrine and paracrine Wnt signaling in CML progenitors in the context of the bone marrow microenvironment (BMM).[54] To identify the WNT10B-related axis and the Wnt/β-catenin response in *WNT10B*^{R}-positive cell models, we use a chemical interrogation by LGK974 PORCN-inhibitor. Our results indicate that WNT10B^{IVS1} gene silencing by shRNA or treatment with the PORCN inhibitor LGK974 in MOLT-4 and MUTZ2 reduces WNT10B/FZD6 interactions and response in a dose-dependent manner. Contrary to our expectations, exposure to the PORCN inhibitor LGK974 at low doses show the ability to induce a dramatic reduction in WNT10B^{IVS1} mRNA and protein expression, likely by a specific mRNA degradation in response to pharmacologically induced defect in the secretory machinery, thus causing the accumulation of non-secreted protein[55,56]. Furthermore, knocking down WNT10B by shRNA or blocking its PORCN-dependent secretion affect the assayed CTNNB1 (β-catenin), AXIN2, and PYGO2 at transcript level, which suggests the induction of regulatory feedback events. Consistent with this hypothesis, the expression of Wntless (Wls), another component of the Wnt secretion machinery, correlates significantly with the CTNNB1 (β-catenin) mRNA expression levels.[45] In addition, to further confirm the major role of FZD6 in WNT10B-mediated activation, the expression of FZD6 has been interfered by the A83-01, a TGF-βRI inhibitor, via inhibiting TGF-β1-induced SMAD2 phosphorylation that down-regulates FZD6 expression as previously reported.[35] Through LGK974 exposure and A83-01-mediated down-regulation, we revealed here that FZD6 is a positive regulator of the WNT10B-mediated β-catenin-dependent signaling. A previous study showed that the stimulation of TGF-β increased the production of the WNT10B, due to a potential cooperative function of SMAD and NFAT in the induction of WNT10B gene expression.[57] *WNT10B* gene promoter region organization suggests that its transcription is regulated by the binding of NFAT/SMAD3 dimers.[41] Notably, our data show that A83-01 exposure did not significantly inhibit WNT10B^{IVS1} expression despite the interference of the SMAD-inducer TGF-β was expected

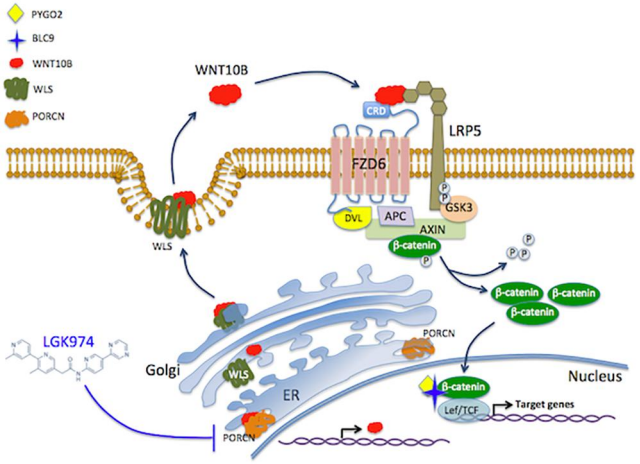

FIGURE 7 A speculative model of WNT10B and FZD6 synergy. WNT10B binds to FZD6 (and potentially to FZD4 and FZD5 with a minor extent, not shown in the model for the sake of simplicity) and signals to stabilize β-catenin. Porcupine (PORCN) is a membrane-bound *O*-acyl transferase that is required for the palmitoylation of Wnt proteins and that is essential in diverse Wnt pathways for Wnt-Wntless (WLS) binding, Wnt secretion, and Wnt signaling activity. LGK974 strongly inhibited Wnt secretion in MOLT4 and MUTZ2 cells expressing the WNT10B^{IVS1} allelic variant

and has been here observed for the TGFβ-dependent WNT10B expression in the control HeLa cells.[57]

5 | CONCLUSIONS

In summary, we show in this study that FZD6 plays a crucial role in the WNT10B-mediated β-catenin-dependent Wnt signaling activation in *WNT10B*^{R}-positive cells. Both *TCF7* and *LEF1* transcription factors are overexpressed in T-ALL patients and in MOLT4 cell line but not in MUTZ2 AML cell model, in accordance with previous observations.[16,58] Mechanistically, FZD6-WNT10B complex is a positive regulator that promotes Wnt/β-catenin pathway, a signaling previously demonstrated to support stem cell function in T-ALL.[26] Indeed, leukemic Wnt/β-catenin pathway is supported by the WNT10B misregulated function and is successfully druggable by the potent PORCN inhibitor LGK974. We showed compelling evidence for a dose-dependent inhibition of FZD6-WNT10B complex formation in vitro, dramatic down-modulation of WNT10B^{IVS1} transcript, and identification of potential genetic markers to enrich for leukemias that are responsive to LGK974. A speculative model is presented in Figure 7. By altering FZD6-WNT10B complex formation, the basis for therapeutic strategies to target leukemic stem cells in leukemic patients can be provided.

ACKNOWLEDGMENTS

The authors thank Dr. Lazzaroni F. for the experimental support, Dr. Crucitti L. (Grande Ospedale Metropolitano Niguarda, Milano) and Dr. Cassin R. (Ospedale Maggiore Policlinico, Milano) for the support with the clinical database; Dr. Pezzetti L. (Grande Ospedale Metropolitano Niguarda) for assistance with the cell bank; Dr. Brusamolino R. for helpful discussion and Fondazione Malattie del Sangue Onlus (FMS, Dr. Morra E.) for the continuous support. This work was supported by a Grant of the FRRB (Fondazione Regionale per la Ricerca Biomedica) [FRRB 2015]; the Novartis Pharma funding [2017] and LGK974 drug supply; and the support of Lions club Milano Host (2017).

CONFLICT OF INTEREST

The authors declare no conflict of interest. The funders had no role in the design of the study; in the collection, analyses, or interpretation of data; in the writing of the manuscript or in the decision to publish the results.

AUTHOR CONTRIBUTIONS

Conceptualization: Alessandro Beghini; Methodology: Alessandro Beghini and Adriana Cassaro; Formal analysis: Barbara di Camillo, Giorgio Valentini, Marco Notaro, and Jessica Gliozzo; Investigation: Adriana Cassaro, Ilaria Esposito, and Alessandra Trojani; Resources: Giovanni Grillo, Roberto Cairoli, and Gianluigi Reda; Funding acquisition: Roberto Cairoli, and Alessandro Beghini; Writing: Alessandro Beghini.

INSTITUTIONAL REVIEW BOARD STATEMENT

The study was conducted according to the guidelines of the Declaration of Helsinki, and approved by the Ethics Committee of Grande Ospedale Metropolitano Niguarda (N°19-22.06.2018).

INFORMED CONSENT STATEMENT

Informed consent was obtained from all subjects involved in the study.

DATA AVAILABILITY STATEMENT

The NGS data presented in this study are openly available in Gene Express Omnibus at [https://www.ncbi.nlm.nih.gov/geo/query/acc.cgi?acc=GSE159797], reference number [*GSE159797*].

ORCID

Alessandro Beghini https://orcid.org/0000-0002-8234-3474

PEER REVIEW

The peer review history for this article is available at https://publons.com/publon/10.1002/hon.2840.

REFERENCES

1. Aifantis I, Raetz E, Buonamici S. Molecular pathogenesis of T-cell leukaemia and lymphoma. *Nat Rev Immunol*. 2008;8:380-390.
2. You MJ, Medeiros LJ, Hsi ED. T-lymphoblastic leukemia/lymphoma. *Am J Clin Pathol*. 2015;144:411-422.
3. Pui C-H, Evans WE. Treatment of acute lymphoblastic leukemia. *N Engl J Med*. 2006;354:166-178.
4. Zúñiga-Pflücker JC. T-cell development made simple. *Nat Rev Immunol*. 2004;4:67-72.
5. Hosokawa H, Rothenberg EV. Cytokines, transcription factors, and the initiation of T-cell development. *Cold Spring Harb Perspect Biol*. 2018;10:a028621
6. Weerkamp F, van Dongen JJM, Staal FJT. Notch and Wnt signaling in T-lymphocyte development and acute lymphoblastic leukemia. *Leukemia*. 2006;20:1197-1205.
7. Rothenberg EV, Moore JE, Yui MA. Launching the T-cell-lineage developmental programme. *Nat Rev Immunol*. 2008;8:9-21.
8. Gattinoni L, Zhong X-S, Palmer DC, et al. Wnt signaling arrests effector T cell differentiation and generates CD8+ memory stem cells. *Nat Med*. 2009;15:808-813.
9. Katoh M. Canonical and non-canonical WNT signaling in cancer stem cells and their niches: cellular heterogeneity, omics reprogramming, targeted therapy and tumor plasticity (Review). *Int J Oncol*. 2017;51:1357-1369.
10. Staal FJT, Clevers HC. Wnt signaling and haematopoiesis: a Wnt-Wnt situation. *Nat Rev Immunol*. 2005;5:2130.
11. Hendriksen J, Jansen M, Brown CM, et al. Plasma membrane recruitment of dephosphorylated Î²-catenin upon activation of the Wnt pathway. *J Cell Sci*. 2008;121:1793-1802.
12. Clevers H, Nusse R. Wnt/Î²-catenin signaling and disease. *Cell*. 2012;149:1192-1205.
13. MacDonald BT, Tamai K, He X. Wnt/Î²-catenin signaling: components, mechanisms, and diseases. *Dev Cell*. 2009;17:9-26.
14. Nakamura Y, de Paiva Alves E, Veenstra GJ, et al. Tissue- and stage specific Wnt target gene expression is controlled subsequent to Î²-catenin recruitment to cis-regulatory modules. *Development*. 2016;143(11):1914-1925.

15. Nakamura Y, Hoppler S. Genome-wide analysis of canonical Wnt target gene regulation in Xenopus tropicalis challenges Î²-catenin paradigm. *Genesis*. 2017;55(1-2).e22991.
16. Ng OH, Erbilgin Y, Firtina S, et al. Deregulated Wnt signaling in childhood T-cell acute lymphoblastic leukemia. *Blood Cancer J*. 2014; 4.e192.
17. Soares-Lima SC, Pombo-de-Olivera MS, Carneiro FRG. The multiple ways Wnt signaling contributes to acute leukemia pathogenesis. *J Leukocyte Biol*. 2020:1-19. https://doi.org/10.1002/JLB.2MR0420-707R.
18. Nusse R, Clevers H. Wnt/Î²-catenin signaling, disease, and emerging therapeutic modalities. *Cell*. 2017;169:985-999.
19. Weerkamp F, Baert MRM, Naber BAE, et al. Wnt signaling in the thymus is regulated by differential expression of intracellular signaling molecules. *Proc Natl Acad Sci*. 2006;103:3322-3326.
20. Staal FJT, Arens R. Wnt signaling as master regulator of T-lymphocyte responses: implications for transplant therapy. *Transplantation*. 2016;1:2584-2592.
21. Pacifici R. Role of T cells in the modulation of PTH action: physiological and clinical significance. *Endocrine*. 2013;44:576-582.
22. Luis TC, Naber BAE, Roozen PPC, et al. Canonical Wnt signaling regulates hematopoiesis in a dosage-dependent fashion. *Cell Stem Cell*. 2011;9:345-356.
23. Reya T, Duncan AW, Ailles L, et al. A role for Wnt signalling in self-renewal of haematopoietic stem cells. *Nature*. 2003;423:409-414.
24. Sturgeon CM, Ditadi A, Awong G, Kennedy M, Keller G. Wnt signaling controls the specification of definitive and primitive hematopoiesis from human pluripotent stem cells. *Nat Biotechnol*. 2014;32:554-561.
25. Guo Z, Dose M, Kovalovsky D, et al. -Catenin stabilization stalls the transition from double-positive to single-positive stage and predisposes thymocytes to malignant transformation. *Blood*. 2007;109:5463-5472.
26. Giambra V, Jenkins CE, Lam SH, et al. Leukemia stem cells in T-ALL require active Hif1Î± and Wnt signaling. *Blood*. 2015;125:3917-3927.
27. Lazzaroni F, Del Giacco L, Biasci D, et al. Intronless WNT10B-short variant underlies new recurrent allele-specific rearrangement in acute myeloid leukaemia. *Sci Rep*. 2016. https://doi.org/10.1038/srep37201.
28. Sercan Z, Pehlivan M, Sercan HO. Expression profile of WNT, FZD and sFRP genes in human hematopoietic cells. *Leuk Res*. 2010;34:946-949.
29. Belmonte M, Hoofd C, Weng AP, Giambra V. Targeting leukemia stem cells: which pathways drive self-renewal activity in T-cell acute lymphoblastic leukemia? *Curr Oncol*. 2015;23:34.
30. Dose M, Emmanuel AO, Chaumeil J, et al. Î²-Catenin induces T-cell transformation by promoting genomic instability. *Proc Natl Acad Sci*. 2014;111:391-396.
31. Cox CV, Martin HM, Keams PR, Virgo P, Evely RS, Blair A. Characterization of a progenitor cell population in childhood T-cell acute lymphoblastic leukemia. *Blood*. 2007;109:674-682.
32. Cassaro A, Lazzaroni F, Grillo G, Reda G, Cairoli R, Beghini A. Targeting WNT10B-driven signalling through induction of FZD6 By porcupine inhibition in T cell acute lymphoblastic leukemia. *Blood*. 2019;134:3956-3956.
33. Chen B, Dodge ME, Tang W, et al. Small molecule-mediated disruption of Wnt-dependent signaling in tissue regeneration and cancer. *Nat Chem Biol*. 2009;5:100-107.
34. Liu J, Pan S, Hsieh MH, et al. Targeting Wnt-driven cancer through the inhibition of porcupine by LGK974. *Proc Natl Acad Sci*. 2013;110:20224-20229.
35. Ho Y-S, Tsai W-H, Lin F-C, et al. Cardioprotective actions of TGFÎ²RI inhibition through stimulating autocrine/paracrine of survivin and inhibiting Wnt in cardiac progenitors: a83-01 stimulates survivin and inhibits Wnt in CPC. *Stem Cells*. 2016;34:445-455.
36. Takada R, Satomi Y, Kurata T, et al. Monounsaturated fatty acid modification of Wnt protein: its role in Wnt secretion. *Dev Cell*. 2006;11:791-801.
37. Barrott JJ, Cash GM, Smith AP, Barrow JR, Murtaugh LC. Deletion of mouse PORCN blocks Wnt ligand secretion and reveals an ectodermal etiology of human focal dermal hypoplasia/Goltz syndrome. *Proc Natl Acad Sci*. 2011;108:12752-12757.
38. Herr P, Hausmann G, Basler K. WNT secretion and signalling in human disease. *Trends Mol Med*. 2012;18:483-493.
39. Soneson C, Delorenzi M. A comparison of methods for differential expression analysis of RNA-seq data. *BMC Bioinf*. 2013;14:91.
40. Schurch NJ, Schofield P, Gierlinski M, et al. How many biological replicates are needed in an RNA-seq experiment and which differential expression tool should you use? *RNA*. 2016;22:839-851.
41. Tyagi AM, Yu M, Darby TM, et al. The microbial metabolite butyrate stimulates bone formation via T regulatory cell-mediated regulation of WNT10B expression. *Immunity*. 2018;49:1116-1131.e7.
42. Beghini A, Corlazzoli F, Del Giacco L, et al. Regeneration-associated WNT signaling is activated in long-term reconstituting AC133bright acute myeloid leukemia cells. *Neoplasia*. 2012;14:1236-1248.
43. Khan NI, Bradstock KF, Bendall LJ. Activation of Wnt/Î²-catenin pathway mediates growth and survival in B-cell progenitor acute lymphoblastic leukaemia. *Br J Haematol*. 2007;138:338-348.
44. Luis TC, Ichii M, Brugman MH, Kincade P, Staal FJT. Wnt signaling strength regulates normal hematopoiesis and its deregulation is involved in leukemia development. *Leukemia*. 2016;26:414-421.
45. Chiou S-S, Wang L-T, Huang S-B, et al. Wntless (GPR177) expression correlates with poor prognosis in B-cell precursor acute lymphoblastic leukemia via Wnt signaling. *Carcinogenesis*. 2014;35:2357-2364.
46. Bigas A, Guillen Y, Schoch L, Arambilet D. Revisiting b-catenin signaling in T-cell development and T-cell acute lymphoblastic leukemia. *Bioessays*. 2020;42.1900099
47. Wu Q-L, Zierold C, Ranheim EA. Dysregulation of Frizzled 6 is a critical component of B-cell leukemogenesis in a mouse model of chronic lymphocytic leukemia. *Blood*. 2009;113:3031-3039.
48. Wu S, Zhang W, Shen D, Lu J, Zhao L. PLCB4 upregulation is associated with unfavorable prognosis in pediatric acute myeloid leukemia. *Oncol Lett*. 2019;18:6057-6065.
49. Haider Z, Larsson P, Landfors M, et al. An integrated transcriptome analysis in T-cell acute lymphoblastic leukemia links DNA methylation subgroups to dysregulated TAL1 and ANTP homeobox gene expression. *Cancer Med* 2019;8:311-324.
50. Barreto-Vergas C, Alvarez-Zavala M, Garcia-Chagollan M, Hernandez-Flores G, Aguillar-Lemarroy A, Jave-Suarez LF. WNT7A expression is downregulated in T lymphocytes after T-cell receptor activation due to histon modifications and in T-ALL by DNA methylation. *Arch Immunol Ther Exp*. 2020;68:18.
51. Milani G, Rebora P, Accordi B, et al. Low PKCa expression within the MRD-HR stratum defines a new subgroup of childhood T-ALL with very poor outcome. *Oncotarget*. 2014;5:5234-5245.
52. Kurayoshi M, Yamamoto H, Izumi S, Kikuchi A. Post-translational palmitoylation and glycosylation of Wnt-5a are necessary for its signalling. *Biochem J*. 2007;402:515-523.
53. Janda CY, Waghray D, Levin AM, Thomas C, Garcia KC. Structural basis of Wnt recognition by frizzled. *Science*. 2012;337:59-64.
54. Agarwal P, Zhang B, Ho Y, et al. Enhanced targeting of CML stem and progenitor cells by inhibition of porcupine acyltransferase in combination with TKI. *Blood*. 2017;129:1008-1020.

55. Hollien J, Weissman JS. Decay of endoplasmic reticulum-localized mRNAs during the unfolded protein response. *Science*. 2006;313:104-107.
56. Karamyshev AL, Patrick AE, Karamysheva ZN, et al. Inefficient SRP interaction with a nascent chain triggers a mRNA quality control pathway. *Cell*. 2014;156:146-157.
57. Thacker PC, Karunagaran D. Curcumin and emodin down-regulate TGF-Î² signaling pathway in human cervical cancer cells. *PLOS One*. 2015;10.e0120045
58. Metzeler KH, Heilmeier B, Edmaier KE, et al. High expression of lymphoid enhancer-binding factor-1 (LEF1) is a novel favorable prognostic factor in cytogenetically normal acute myeloid leukemia. *Blood*. 2012;120:2118-2126.

SUPPORTING INFORMATION

Additional supporting information may be found online in the Supporting Information section at the end of this article.

How to cite this article: Cassaro A, Grillo G, Notaro M, et al. FZD6 triggers Wnt–signalling driven by WNT10B^{IVS1} expression and highlights new targets in T-cell acute lymphoblastic leukemia. *Hematol Oncol*. 2021;39(3):364-379. https://doi.org/10.1002/hon.2840